OUTLINE:

- **INSTRUMENTS AND DATA CORRECTION:**
  - ✓ **Atehalometers AE31, AE33**
    - ❖ Working principle and equations
      - o AE31 correction
        1. Weingartner
        2. Virkkula
        3. ……..
        4. ACTRIS
      - o AE33 correction
        1. On-line factor loading
        2. ACTRIS
  - ✓ **Multiangle Absorption Photometer – MAAP**
    - o Absorption“reference” instrument for AE calibration
  - ✓ **Nephelometers TSI AND ECOTECH**
    - ❖ Working principle and equations
      - o Scattering and hemispheric backscattering correction
  - ✓ **PM mass concentration**
    - ❖ TEOM, GRIMM

- **DATA INTERPRETATION:**
  - ✓ **Extensive aerosol particle optical properties**
    - ❖ Scattering and hemispheric backscattering
    - ❖ Absorption
  - ✓ **Intensive aerosol particle optical properties**
    - ❖ SAE, AAE, SSA, SSA-AE (optical)
    - ❖ MAC and MSE (chemical and physical properties)
  - ✓ **Source apportionment**
    - ❖ Aethalometer model: fossil vs. non-fossil

- **CALCULATIONS:**
  - ✓ **XLS templates**

- **DATA VISUALIZATION:**
  - ✓ **R space**
    - ❖ OPENAIR
    - ❖ FIELDS
    - ❖ ……..

QA/QC

- *Plot raw high-time resolution data*
- *Check outliers*:
    - FLAG data (i.e. contamination, extreme values, known or unknown reasons, extreme negative values….)
- *Check calibration periods*:
    - Remove (put in another file) and FLAG (i.e. missing due to zero/span,..)
- *Check other variables*:
    - i.e. P, T, RH, flow,…..
- *Convert to* standard P (1013.25 hPa) and T (293,15 K) $X_{corr} = X_{uncorr} \left(\frac{P_{ref}}{P}\right)\left(\frac{T}{T_{ref}}\right)$
- *Correct data (i.e. truncation,….)*
- *Calculate hourly averages*

AETHALOMETER 31

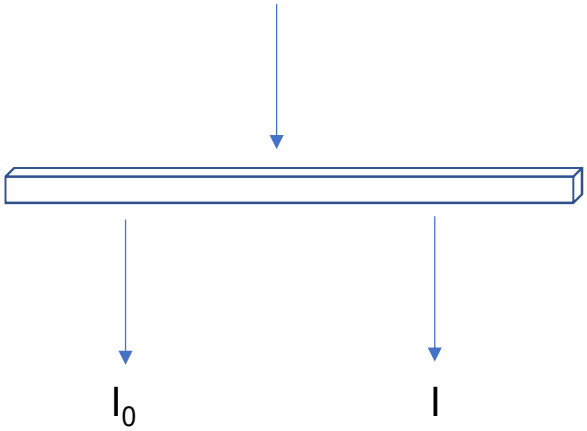

$$ATN = -100 \ln\left(\frac{I}{I_0}\right) \qquad \text{from } I = I_0\, e^{-b_{abs}\cdot x}$$

$$b_{ATN,n} = \frac{A}{Q}\frac{(\mathrm{ATN_n} - \mathrm{ATN_{n\_1}})}{\Delta t} \longrightarrow BC = \frac{1}{\alpha_{ATN}}\frac{A}{Q}\frac{\Delta ATN}{\Delta t} \longrightarrow (b_{ATN} = [BC] \cdot \alpha_{ATN})$$

$$\alpha_{ATN}\left[\frac{m^2}{g}\right] = \frac{14625}{\lambda\,[nm]}$$

(16.6 m^2/g)@880 nm

$$\boldsymbol{b_{abs}(\lambda) = f(b_{ATN}(\lambda))} \;\; \textbf{??}$$

AETHALOMETER 31

ISSUES:

- *Multiple scattering by the filter fibers (the optical path increases);*
- *Scattering of aerosols embedded in the filter (the optical path increases);*
- *Filter loading correction (the optical path reduces).*

$$b_{Abs} = \frac{b_{ATN}}{C \cdot R(ATN)}$$

Weingartner et al. (2003)

Multiple light scattering effects within the filter

Shadowing effect due to filter loading

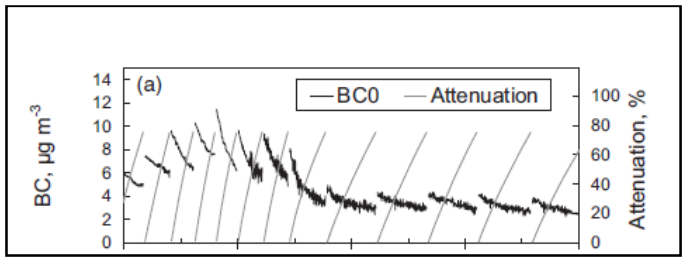

Virkkula et al. (2005)

Do we need to correct our AE31 bATN (λ) data for factor loading (shadowing) ?

A possible approach is based on the idea that within a long enough measurement campaign the probability to measure a certain BC value in an ATN bin is constant and independent of the ATN

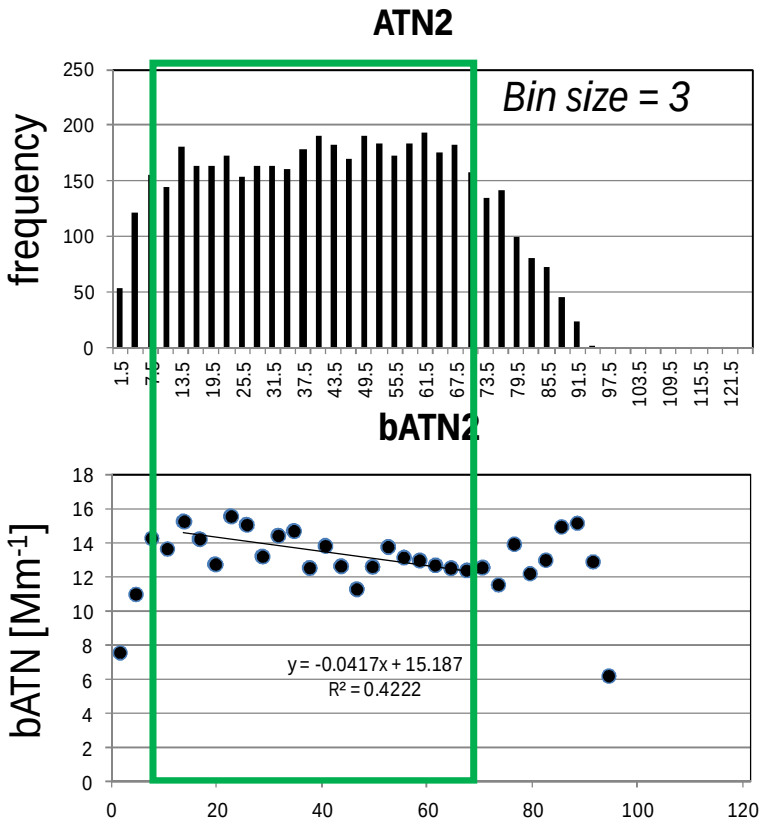

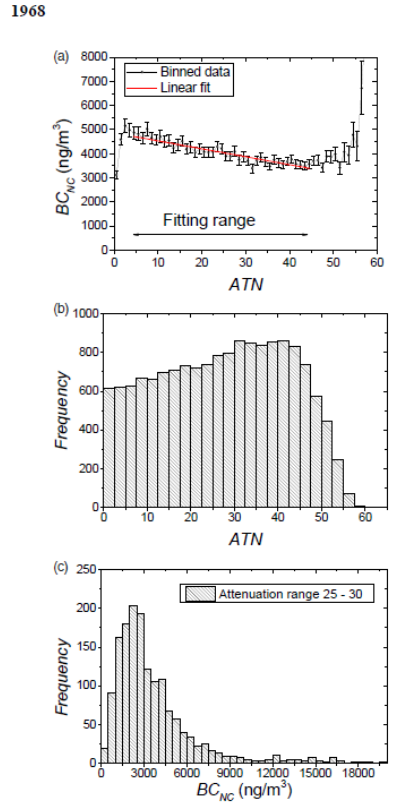

Drinovec et al., AMT, 2015

Figure 2. Example of the analysis of the filter loading effect: BC as a function of ATN. **(a)** BC(ATN) plot: a linear least squares regression in the ATN range 5–45 was used to fit the data. The apparent increase in the plot at ATN = 60 is a statistical artifact. **(b)** Frequency distribution of the number of measurements per ATN bin. **(c)** The BC frequency distribution in the bin 25 < ATN < 30. The measurements were performed in Klagenfurt (Austria) from 1 to 12 March 2012.

AETHALOMETER AE31:

1) Weingartner correction: Determination of C_{ref}

$$b_{abs,n} = \frac{b_{ATN,n}}{C_{ref} \cdot R_{w,n}} = \frac{b_{ATN,n}}{C_{ref} \cdot \left[\left(\frac{1}{f} - 1\right) \cdot \frac{lnATN_n - \ln(10\%)}{\ln(50\%) - \ln(10\%)} + 1\right]}$$

Multiple scattering at the filter fibers

Any other effects that are caused by deposited particles

$$ATN = 0 \rightarrow R_w = 1$$

$$C_{ref} = \frac{b_{ATN=10\%}}{b_{abs,ref}}$$

$$BC = \frac{b_{abs}}{\sigma_{abs}} = \frac{b_{ATN}}{\sigma_{abs} \cdot C_{ref} \cdot R_w}$$

E. Weingartner et al. / Aerosol Science 34 (2003) 1445–1463

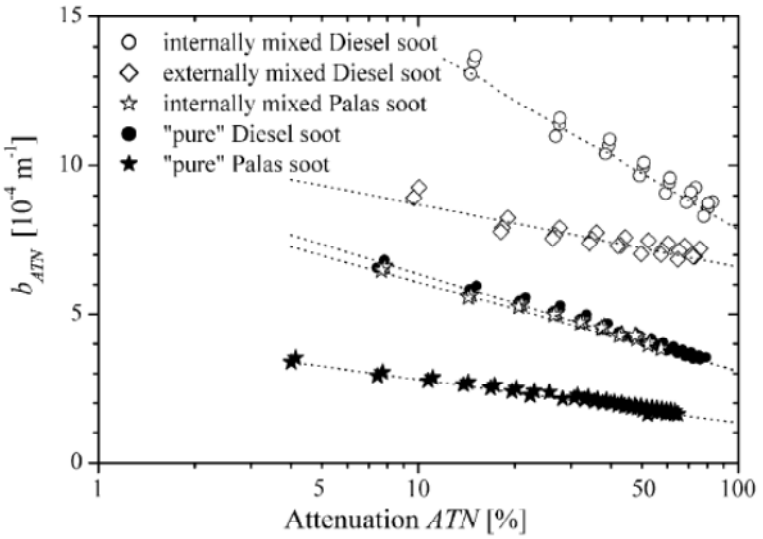

AETHALOMETER AE31:

1) Weingartner correction: Determination of loading factor f at λ-ref (measured $R_{w,n}$)

$$b_{abs,n} = \frac{b_{ATN,n}}{C_{ref} \cdot R_{w,n}} = \frac{b_{ATN,n}}{C_{ref} \cdot \left[\left(\frac{1}{f} - 1\right) \cdot \frac{lnATN_n - \ln(10\%)}{\ln(50\%) - \ln(10\%)} + 1\right]}$$

$$\frac{b_{ATN}^{637}}{C_{Ref} \cdot b_{Abs,ref}^{637}} = \left[\left(\frac{1}{f} - 1\right) \cdot \left(\frac{\ln(ATN) - \ln(10)}{\ln(50) - \ln(10)}\right) + 1\right]$$

$$\underbrace{\frac{b_{ATN}^{637}}{C_{Ref} \cdot b_{Abs,ref}^{637}} - 1}_{y} = \left(\frac{1}{f} - 1\right) \cdot \underbrace{\left(\frac{\ln(ATN) - \ln(10)}{\ln(50) - \ln(10)}\right)}_{x}$$

$$y = \left(\frac{1}{f} - 1\right) \cdot x$$

AETHALOMETER AE31:

1) Weingartner correction: Determination of loading factor f at λ-ref (Single Scattering Albedo)

$$b_{abs,n} = \frac{b_{ATN,n}}{C_{ref} \cdot R_{w,n}} = \frac{b_{ATN,n}}{C_{ref} \cdot \left[\left(\frac{1}{f} - 1\right) \cdot \frac{lnATN_n - \ln(10\%)}{\ln(50\%) - \ln(10\%)} + 1\right]}$$

$$f(\lambda) = m \cdot (1 - \omega_0) + 1$$

$0.85 < m < 0.87$

$$\omega_0 = \frac{Scatt}{Scatt + Abs_{Ref}}$$

AETHALOMETER AE31:

1) Weingartner correction: Determination of loading factor f(λ)

$$b_{abs,n} = \frac{b_{ATN,n}}{C_{ref} \cdot R_{w,n}} = \frac{b_{ATN,n}}{C_{ref} \cdot \left[\left(\frac{1}{f} - 1\right) \cdot \frac{lnATN_n - \ln(10\%)}{\ln(50\%) - \ln(10\%)} + 1\right]}$$

$$b_{ATN,n} = b_{10\%} \cdot R_{w,n}$$ (convert all b_{ATN} values to $b_{10\%}$)

$$b_{ATN}(\lambda) = b_{ATN=10\%}(\lambda) \cdot \left[\left(\frac{1}{f} - 1\right) \cdot \left(\frac{\ln(ATN) - \ln(10)}{\ln(50) - \ln(10)}\right) + 1\right]$$

$$\left(\frac{b_{ATN}(\lambda) - b_{ATN=10\%}(\lambda)}{b_{ATN=10\%}(\lambda)}\right) = \left(\frac{1}{f} - 1\right) \cdot \left(\frac{\ln(ATN) - \ln(10)}{\ln(50) - \ln(10)}\right)$$

AETHALOMETER AE31:

A value for the compensation parameter can be calculated for each filter spot

2) Virkkula correction

$$b_{abs} = \left(k_0 + k_1 \cdot ln\left(\frac{I}{I_0}\right)\right) \cdot b_{ATN} - s \cdot b_{sp}$$

k_0, k_1, s: empirically derived constants

$$= (k_0 + k_1 \cdot ATN) \cdot b_{ATN} - s \cdot b_{sp}$$

$$ATN = 0 \rightarrow BC_{raw} = BC_{true}$$

$$if\ b_{sp}\ is\ not\ available \rightarrow k_0\ and\ s = 1$$

$$b_{abs} = (1 + k \cdot ATN) \cdot b_{ATN}$$

$$BC_{corr} = (1 + k \cdot ATN) \cdot BC_0$$

$$BC_{corr}(t_{i\ last}) = BCcorr(t_{i\ +\ 1\ first})$$

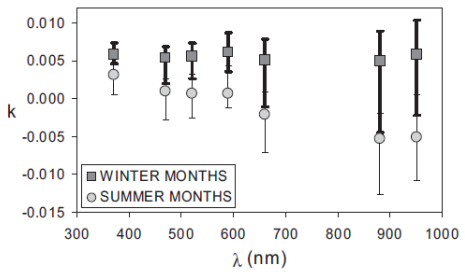

Figure 9. The median factor *k* in winter (November–April) and summer (June–August) at the Hyytiälä station. The error bars contain 95% of the data.

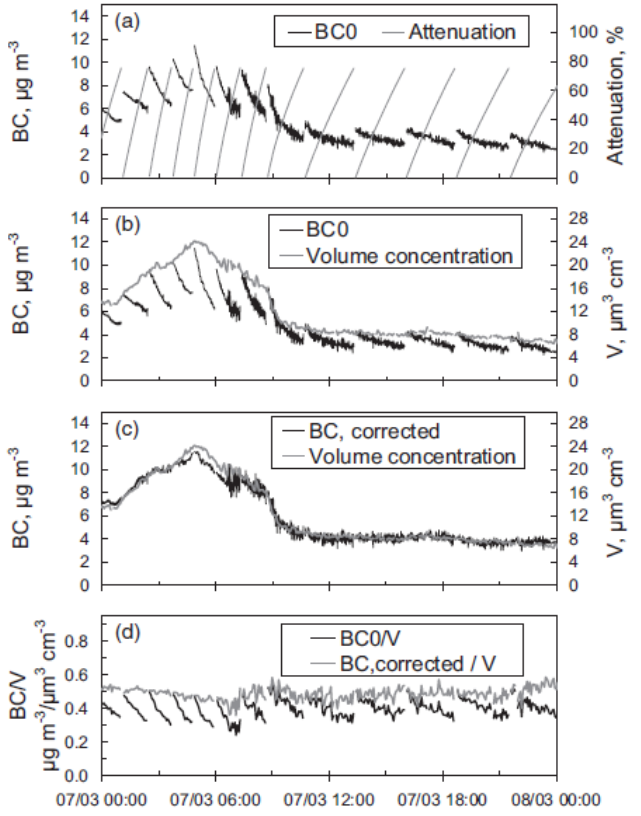

$$k_i = \frac{BC_0(t_{i+1,first}) - BC_0(t_{i,last})}{ATN(t_{i,last}) \cdot BC_0(t_{i,last}) - ATN(t_{i+1,first}) \cdot BC_0(t_{i+1,first})}$$

$$k_i = \frac{1}{ATN(t_{i,last})} \cdot \left(\frac{BC_0(t_{i+1,first})}{BC_0(t_{i,last})} - 1\right)$$

AETHALOMETER AE31:

Montseny station (RB; NE Spain)

2) Virkkula correction

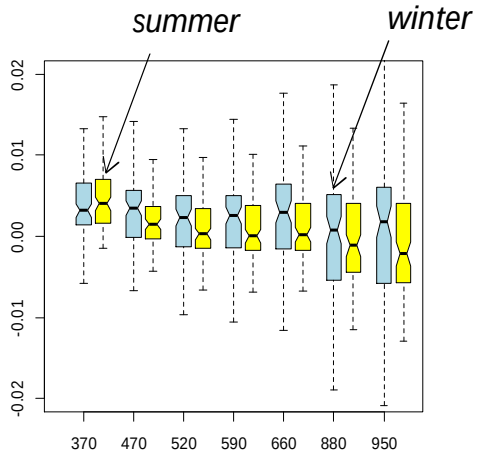

30 min average around filter spot change time

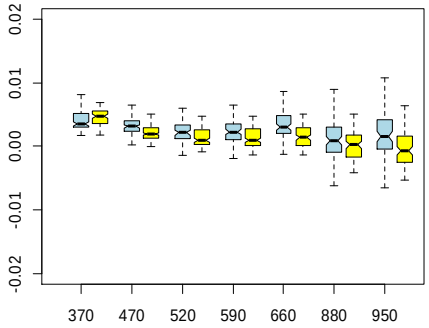

9 filter spot sliding average

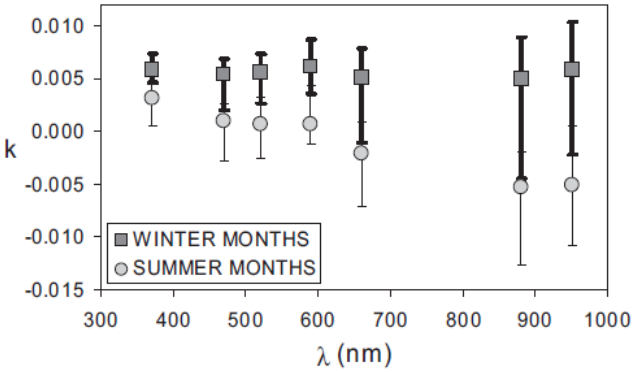

Figure 9. The median factor *k* in winter (November–April) and summer (June–August) at the Hyytiälä station. The error bars contain 95% of the data.

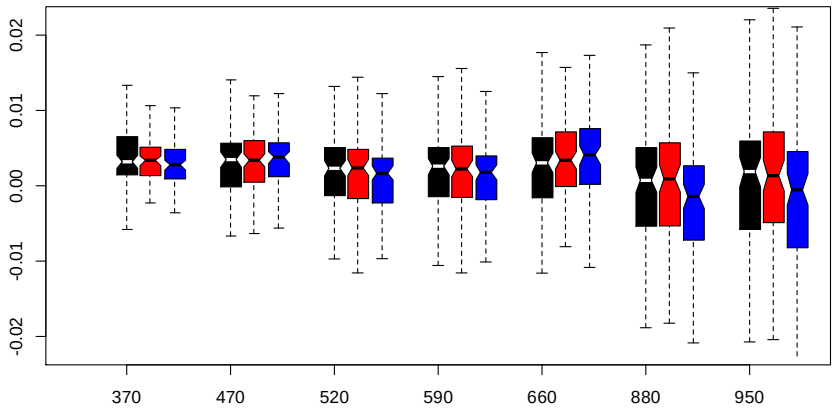

30 min before/after filter spot change

20 min

10 min

AETHALOMETER AE31: **4) SEGURA-WEINGARTNER-SCHMID-ARNOTT** *(Segura et al., 2015)*

- Application of Weingartner scheme to determine ***f*** and C_{637nm};

- C(λ) was studied using the *Schmid et al. (2006)* parameterization:

$$C(\lambda) = C^*(\lambda) + m_s(\lambda) \cdot \frac{\omega_0(\lambda)}{1 - \omega_0(\lambda)}$$

m_s (Arnott et al., 2005) is the fracion of aerosol scattering coefficient erroneously interpreted as absorption

- SEGURA used $m_s(\lambda)$ from *Arnott et al. (2005)* and used the same λ-dependence of C(λ) from *Arnott et al. (2005)*.

- Calculate C^*_{637nm} and then C(λ) using the same λ-dependence of C(λ) as in Schmid et al. (2006) with the following formula:

$$C(\lambda) = C^*(\lambda) + m_s(\lambda) \cdot \left[\frac{\omega_0^{637} \cdot \left(\frac{\lambda}{637}\right)^{-SAE}}{\omega_0^{637} \cdot \left(\frac{\lambda}{637}\right)^{-SAE} + (1 - \omega_0^{637}) \cdot \left(\frac{\lambda}{637}\right)^{-AAE}} \right]$$

- Application of an iterative procedure:

  - Use bATN-AE to calculate C(λ) first guess; use it in $b_{abs}(\lambda) = \frac{b_{ATN}(\lambda)}{C(\lambda) \cdot R(f, ATN)}$
  - Calculate bABS-AE to calculate C(λ) second guess; use it in the formula above;
  - Continue up to convergence of bABS-AAE.

AETHALOMETER AE33:

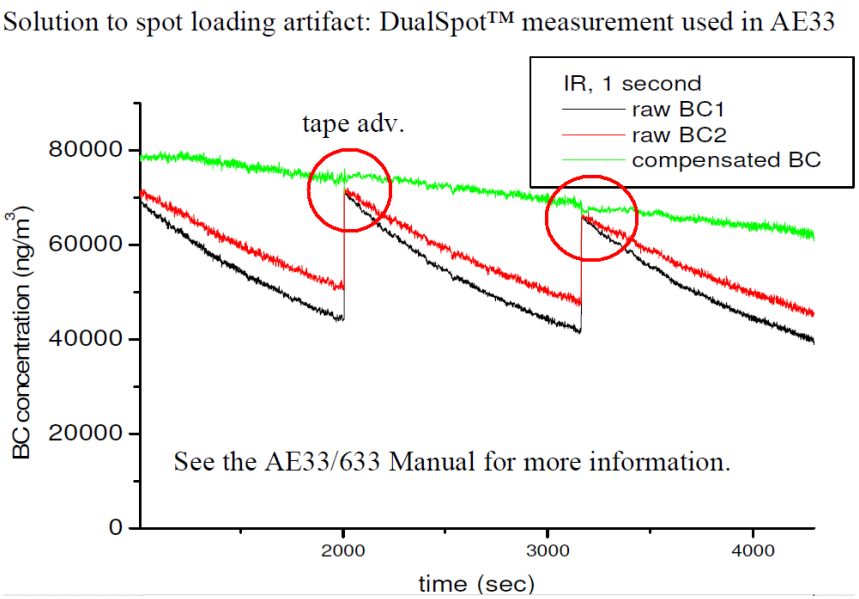

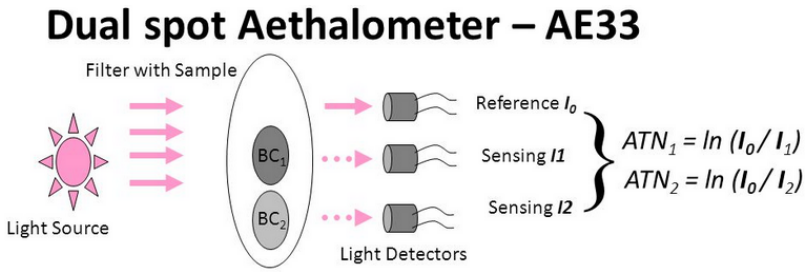

- The K loading correction factor is generated dynamically by the AE33 from 2 spot data.
- One K value for each channel (K1,……,K7)

$$BC = \frac{BC_{NC}}{C \cdot (1 - K \cdot ATN)}$$

$$\begin{cases} e^{-\sigma K B_1} = (1 - K \cdot ATN_1) \\ e^{-\sigma K B_2} = (1 - K \cdot ATN_2) \end{cases} \longrightarrow y = \frac{ln(1 - K \cdot ATN_2)}{ln(1 - K \cdot ATN_1)}$$

Same aerosol collected with different rates:
different loadings but same K value

AETHALOMETER AE31 and AE33: *credits to Thomas Müller, Leibniz Institute for Tropospheric Research, Leipzig*

3) ACTRIS correction

$$b_{abs} = \frac{b_{ATN}}{C_0}$$

$$ATN = -100 \ln\left(\frac{I}{I_0}\right)$$

$$b_{ATN,n} = \frac{1}{100}\frac{A}{Q}\frac{\Delta \mathrm{ATN}}{\Delta t}$$

The attenuation coefficient is calculated from eBC concentration by

AE31

$$b_{ATN} = [eBC] \cdot \alpha_{ATN}$$

AE33

TFE-coated glass fiber filter

$$b_{ATN} = [eBC] \cdot k(ATN) \cdot \alpha_{ATN} \cdot k(ATN) \cdot \frac{1.57}{2.14}$$

Quartz fiber filter

AETHALOMETER AE31: *credits to Thomas Müller, Leibniz Institute for Tropospheric Research, Leipzig*

3) ACTRIS correction

$$b_{abs} = \frac{b_{ATN} - b_{sca} \cdot [(s_0 - s_1 g) \cdot e^{(-(s_2 - s_3 g)ATN)} + s_4]}{C_0 + C_1 \cdot ATN}$$

C_1 = 0.0147, S_0 = 0,1060, S_1 = 0.1309, S_2 = 0.0649, S_3 = -0.1524, S_4 = 0.0072

$$C_0 = \frac{b_{ATN} - b_{sca} \cdot \left[(s_0 - s_1 \cdot g) \cdot e^{(-(s_2 - s_3 \cdot g) \cdot ATN)} + s_4\right] - b_{abs,ref} \cdot c_1 \cdot ATN}{b_{abs,ref}}$$

$$C_0 = \frac{b_{ATN}}{b_{abs,ref}} - C_1 \cdot ATN$$

$$b_{\mathrm{Abs}} = \frac{b_{ATN}}{C_0 + C_1 \cdot ATN}$$

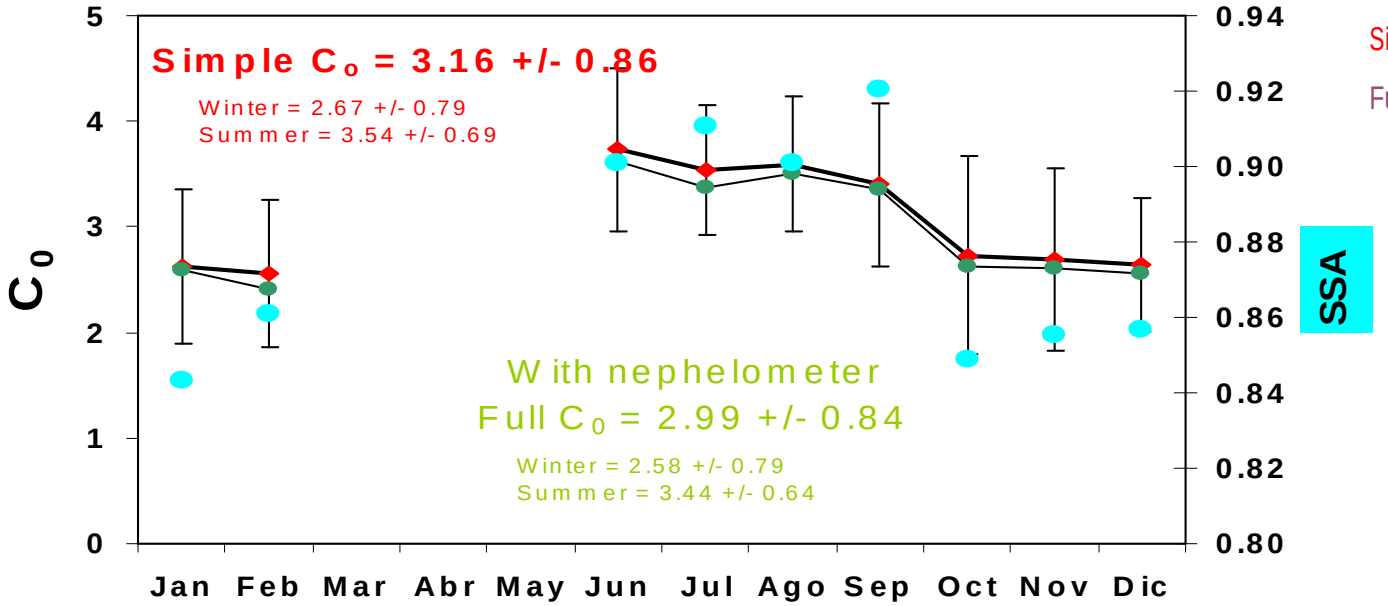

Simple C_0 = without nephelometer data

Full C_0 = with nephelometer data

Montseny station (NE Spain)

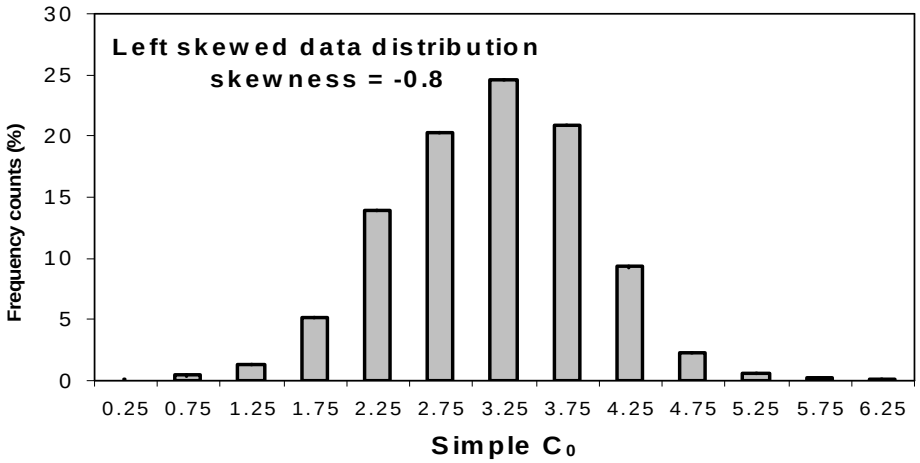

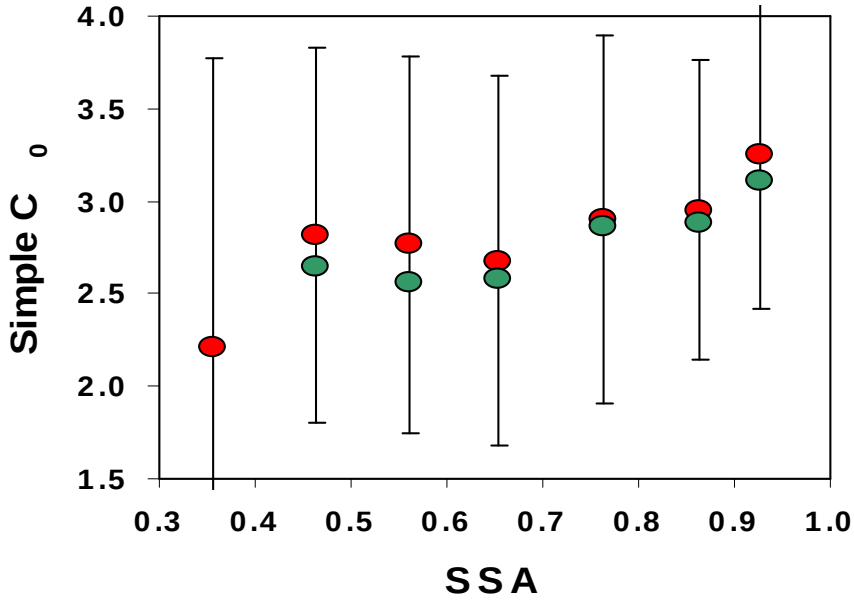

AE31 correction: C_0 values from eight stations

credits to Thomas Müller, TROPOS, Leipzig

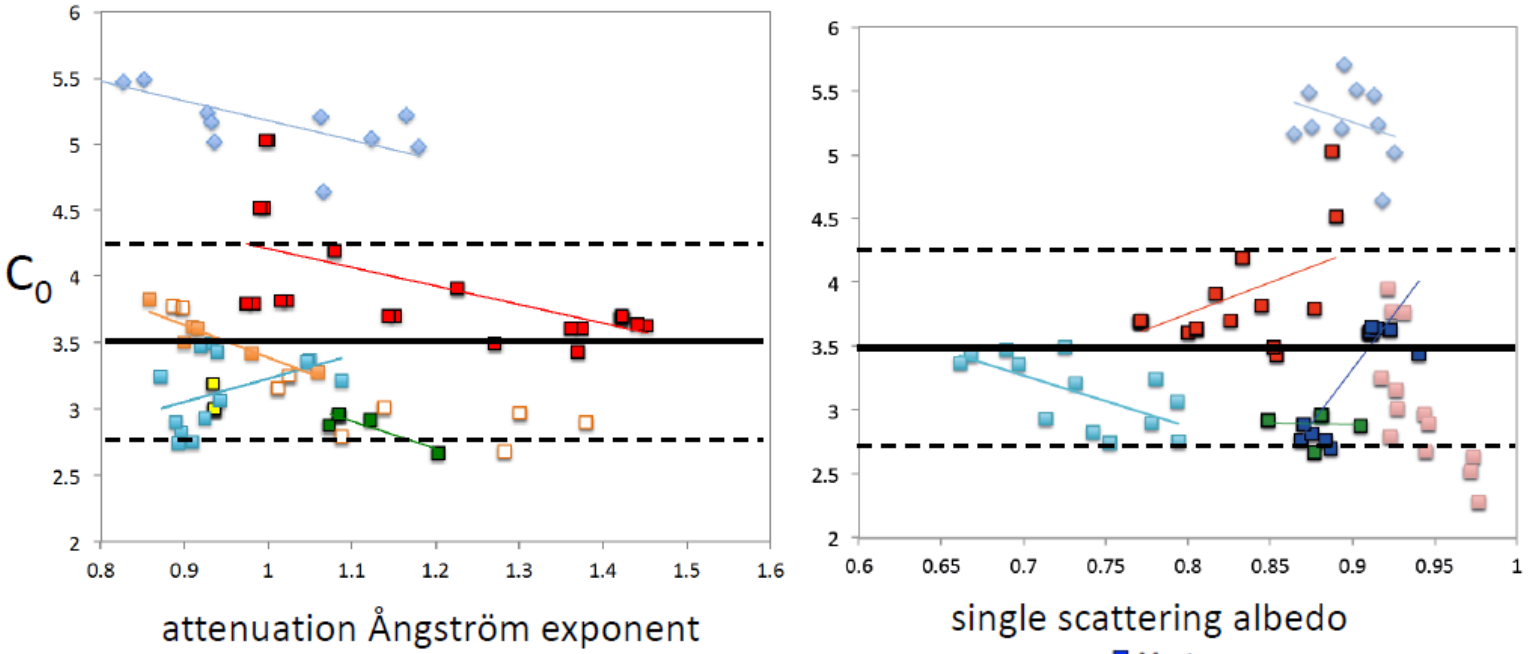

Recommended value: C_0=3.5 ± 0.875 (25%)

AE31 correction: wavelength dependence of correction factors C_0

credits to Thomas Müller, TROPOS, Leipzig

Screen shots from DAQ system

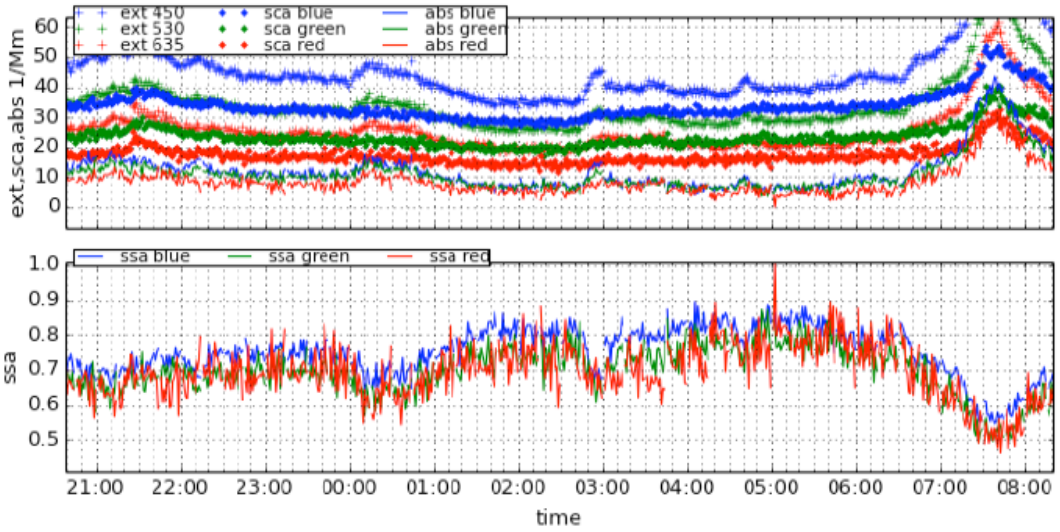

AE31 vs. reference @660 nm

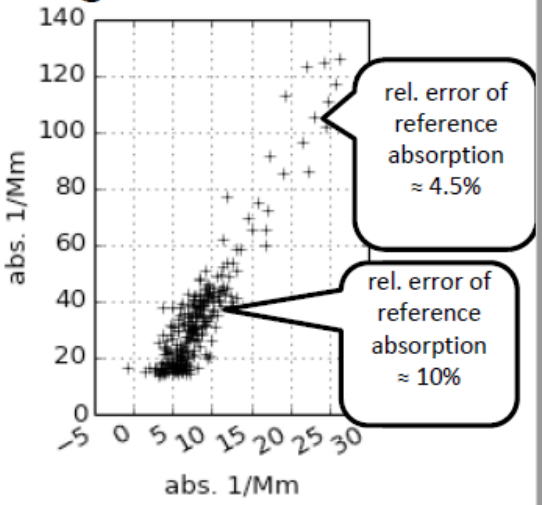

Correction factors C_0

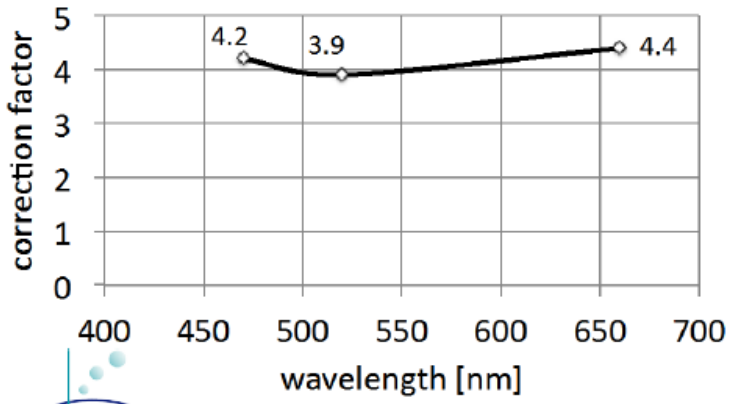

- C_0 varies by about 10% in the wavelength range from 470 to 660 nm
- **Variation in wavelength dependence is small compared to uncertainty of C_0** (25%)

TROPOS
Leibniz Institute for Tropospheric Research

AE33 correction: Wavelength dependence of eBC and C_0

credits to Thomas Müller, TROPOS, Leipzig

eBC concentration of AE33 compared to MAAP

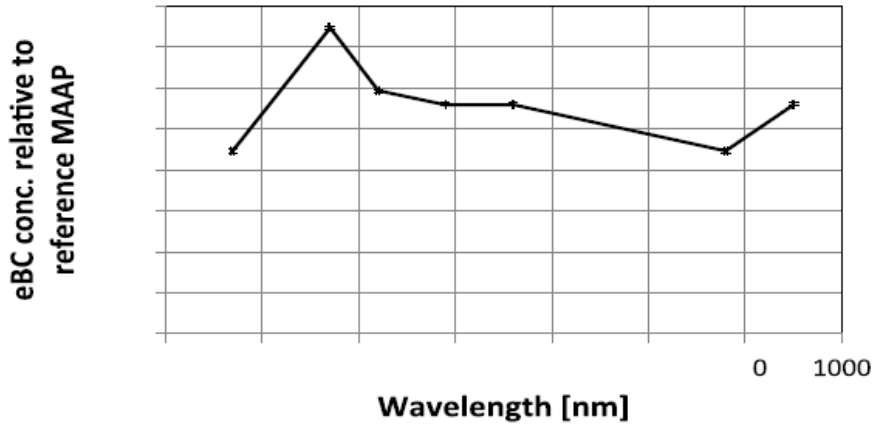

$$b_{Abs} = b_{ATN}\left(\frac{1.57}{3.2}\right)$$

C_0 values derived by comparing absorption coefficients from AE33 and the absorption reference system

wavelength	470 nm	520 nm	660 nm
C_0	3.29 ± 0.014	3.13 ±0.013	3.21±0.02
R^2	0.954	0.954	0.887

AE33: K and aerosol aging

ineris-00971212, version 1

Indication of aerosol aging by optical absorption properties

Luka Drinovec , Grisa Mocnik , Jean-Eudes Petit [1, 2] , Jean Sciare [2] , Olivier Favez [1] , Peter Zotter , Robert Wolf , André S.H. Prevot , Anthony D.A. Hansen Détails

1 INERIS - Institut National de l'Environnement Industriel et des Risques
2 LSCE - Laboratoire des Sciences du Climat et de l'Environnement [Gif-sur-Yvette]

Abstract : The ability to discriminate between local and regional air pollution is important for aerosol monitoring and control. Aging by atmospheric processing can change the aerosol's chemical and physical characteristics. Here we present a new method for indicating aerosol age using optical absorption parameters measured by the dual-spot Aethalometer (Magee Scientific, Model AE33). This instrument provides a real-time determination of a sample-on-filter loading effect, based on the linear model similar to Virkkula (2007) and Park (2010): BC_measured = BC_ambient (1- k*ATN). The compensation parameter k is determined in real-time for each of the operational wavelengths from 370 nm to 950 nm. The wavelength dependence of absorption and the compensation parameter both provide a highly time-resolved specific spectral fingerprint that may be interpreted in terms of aerosol composition in terms of aerosol sources and age. Optical and chemical properties of aerosols were measured with high time resolution during summer and winter EMEP campaigns in Paris (France) and Payerne (Switzerland). An Aerosol Chemical Speciation Monitor (Aerodyne, ACSM) and an High Resolution Time-of-Flight Aerosol Mass Spectrometer (Aerodyne, AMS) were used to measure quantitative chemical composition for non-refractory aerosol particles. During summer we observed complex temporal variation of k, where k(880 nm) changed from approximately 0.006 for fresh aerosols to near zero for aged aerosols as shown using Potential Source Contribution Function (PSCF) back trajectory analysis method. We have combined the Aethalometer and ACSM/AMS measurements, and normalized the sum of inorganic secondary and organic aerosol mass to BC. Values of this ratio are expected to be high for air parcels containing aged aerosols. The ratio correlates well with the loading compensation parameter k measured by the Aethalometer at 880 nm. This indicates that the compensation parameter k can be used for discrimination between local (fresh) and regional (aged) air pollution aerosols.

Type de document : Communication dans un congrès
32. AAAR Annual Conference, Sep 2013, Portland, United States

Domaine : Sciences de l'environnement

The filter-loading effect depends on the optical properties of particles present in the filter matrix, especially on the black carbon particle coating

AETHALOMETER MODEL (wb vs. ff)

$$\begin{cases} \dfrac{Abs(370\,nm)_{ff}}{Abs(950\,nm)_{ff}} = \left(\dfrac{370}{950}\right)^{-AAE_{ff}} \\ \dfrac{Abs(370\,nm)_{wb}}{Abs(950\,nm)_{wb}} = \left(\dfrac{370}{950}\right)^{-AAE_{wb}} \\ Abs(\lambda) = Abs(\lambda)_{ff} + Abs(\lambda)_{wb} \end{cases}$$

$$A = \left(\frac{370}{950}\right)^{-AAE_{ff}}$$

$$B = \left(\frac{370}{950}\right)^{-AAE_{wb}}$$

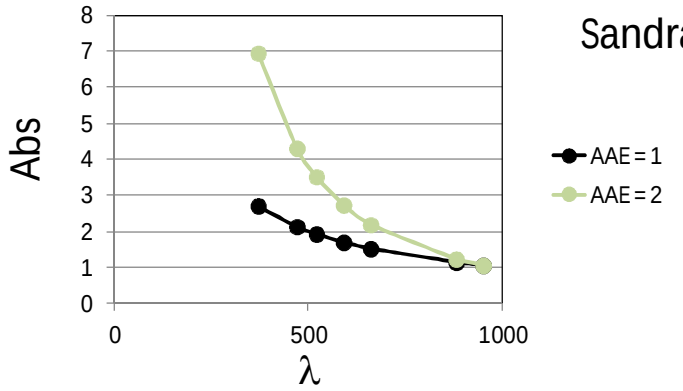

Sandradewi et al., 2008

$$Abs(370nm)_{ff} = \frac{A \cdot (Abs(950nm) - \left(\frac{1}{B}\right) \cdot Abs(370nm))}{\left(1 - \frac{A}{B}\right)}$$

$$Abs(950nm)_{ff} = \frac{Abs(370nm)_{ff}}{A}$$

$$Abs(370nm)_{wb} = Abs(370nm) - Abs(370nm)_{ff}$$

$$Abs(950nm)_{wb} = \frac{Abs(370nm)_{wb}}{B}$$

PSAP

Particle Soot Absorption Photometer (Bond et al., 1999; Ogren, 2010)

$$\sigma_{ap}' = \frac{A}{V} ln\left(\frac{I_0}{I}\right)$$

A = area of the sample spot (0.1783 cm^2)
V = volume of air (cm^3)
I_0 = I(t)
I = I(t+Δt)

$$\sigma_{PSAP} = \frac{\sigma_{ap}'}{1.0796 \cdot \tau + 0.71}$$

τ= filter transmission (=1 for unloaded filter)

Value actually reported by the PSAP

Account for magnification of absorption by filter medium and filter loading

$$\sigma_{adj} = \sigma_{PSAP} \cdot F_{flow} \cdot F_{spot}$$

Deviation from true flow (spot) and PSAP flow (spot)

$$\frac{Q_{PSAP}}{Q_{true}} \qquad \frac{A_{true}}{A_{ref}}$$

The parameters of the B1999 PSAP correction scheme are based on this equation

5.1 mm diameter; spot area of the manufacturer's reference PSAP measured by B1999

PSAP

Particle Soot Absorption Photometer (Bond et al., 1999; Ogren, 2010)

A more intuitive definition of the adjusted absorption is:

$$\sigma^*_{adj} = \left(\frac{Q_{PSAP}}{Q_{true}}\right) \cdot \left(\frac{A_{true}}{A_{PSAP}}\right) \cdot \sigma_{PSAP}$$

Involving only the *true* values and the values used internally in the instrument

$$\sigma_{adj} = \left(\frac{A_{PSAP}}{A_{ref}}\right) \cdot \sigma^*_{adj} = \left(\frac{17.83}{20.43}\right) \cdot \sigma^*_{adj} = 0.873 \cdot \sigma^*_{adj}$$

Filter spot area used internally by the PSAP

Measured spot area of the reference PSAP (=3.14*(5.1/2)^2)

$$\sigma_{adj} = 0.873 \cdot \sigma^*_{adj} = K_1 \cdot \sigma_{sp} + K_2 \cdot \sigma_{ap}$$

The parameters of the B1999 PSAP correction scheme (B1999, Equations (1) and (12)) are based on this equation.

The instrumental response is a linear function of both the absorption coefficient and the scattering coefficient.
Ideal absorption measurement: $K_1 = 0$; $K_2 = 1$

K_1 and K_2 can be determined with a simple multiple linear regression
or (better) with a weighted-least-squares method (to take into account errors and variability associated with σ_{sp} and σ_{ap}).

Equations (1) and (2) yield the same result and are equally valid, the only difference being whether the spot area of the PSAP firmware (*APSAP = 17.83 mm2) or the manufacturer's* reference PSAP (*Aref = 20.43 mm2) is used in the calculation.
.

PSAP

Particle Soot Absorption Photometer

(1) $$\sigma_{ap} = 0.873 \cdot \left(\frac{Q_{PSAP}}{Q_{true}}\right) \cdot \left(\frac{A_{true}}{A_{PSAP}}\right) \cdot \frac{\sigma_{PSAP}}{K_2} - \frac{K_1}{K_2} \cdot \sigma_{sp}$$

Based on alternative definition for the spot size adjustment

(2) $$\sigma_{ap} = \left(\frac{Q_{PSAP}}{Q_{true}}\right) \cdot \left(\frac{A_{true}}{A_{ref}}\right) \cdot \frac{\sigma_{PSAP}}{K_2} - \frac{K_1}{K_2} \cdot \sigma_{sp}$$

From Bond et al. (1999)

Modern PSAP's allow adjustment of the filter area A_{PSAP} in the instrument setup screen (use eq. 1)

$$\epsilon_{slope}\ [Mm^{-1}] = 0.06 \cdot \sigma_{ap,meas}$$

$$\sigma_{ap} = \frac{\sigma_{adj} - K_1 \cdot \sigma_{sp} + \epsilon_{slope} + \epsilon_{noise}}{K_2}$$

$$\epsilon_{noise}\ [Mm^{-1}] = 0.18 \cdot \sqrt{\frac{\tau_0}{\tau}}$$

TABLE 4. Response of instruments to scattering and absorption. The number of tests for each comparison and the r^2 for each analysis are included. The uncertainties bound a 95% confidence interval and include the standard error from the least-squares analysis, as well as possible systematic uncertainties in the reference absorption.

Instrument	K_1^*	K_2^{**}	N	r^2
PSAP	0.02 ± 0.02	1.22 ± 0.11	63	0.94
IP, adjusted to 550 nm	0.09 ± 0.03	1.23 ± 0.13	24	0.91
HIPS	0.04 ± 0.04	1.33 ± 0.26	25	0.82

*Values of $K_1 > 0$ indicate a response to scattering. For ease of use, these values have been determined using nephelometer data that are not corrected for angular nonidealities.

**Values of $K_2 > 1$ indicate an exaggeration of absorption even after correction for the response to scattering.

PSAP

Particle Soot Absorption Photometer

Wavelength adjustment is needed !

(1) $$\sigma_{ap} = 0.873 \cdot \left(\frac{Q_{PSAP}}{Q_{true}}\right) \cdot \left(\frac{A_{true}}{A_{PSAP}}\right) \cdot \frac{\sigma_{PSAP}}{K_2} - \frac{K_1}{K_2} \cdot \sigma_{sp}$$

574 nm

550 nm (TSI, 3-λ) or 525 nm (Ecotech; 3-λ); or 550 nm (OEC; 1-λ)

Solutions:

A) Calculate the scattering at 574 nm using calculated SAE from 3-λ nephelometer;
B) Calculate σ_{ap} at 550 nm using the adidtional following multiplicative factor:

$$\frac{\sigma_{PSAP}[574]}{\sigma_{PSAP}[550]} = \left(\frac{574}{550}\right)^{-AAE}$$

AAE = 1; 0.957
AAE = 0.5; 0.979

NEPHELOMETERS

- *Angular sensitivity of nephelometers: non-Lambertian (non ideal) illumination and angular truncation*

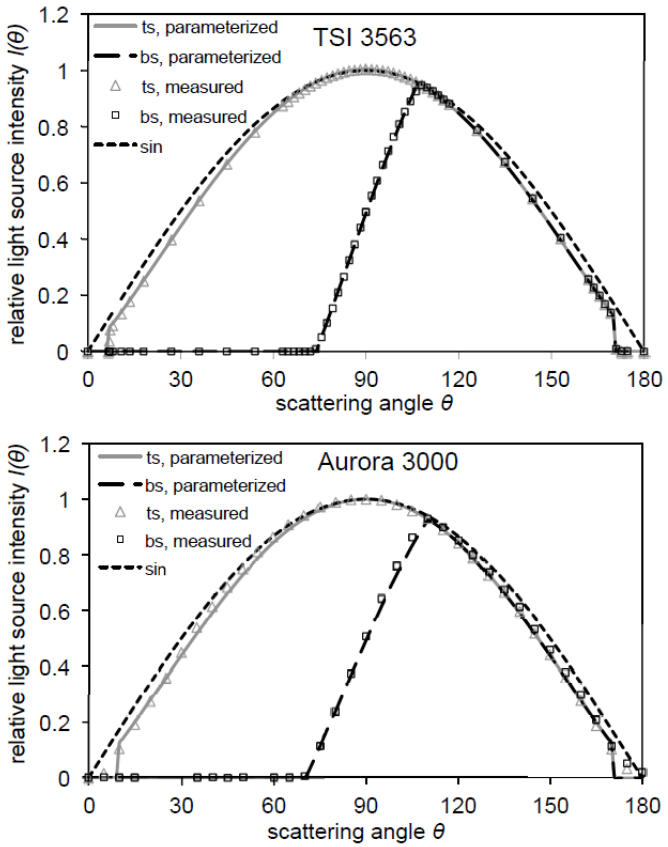

Fig. 3. Measured and parameterized angular intensity functions,

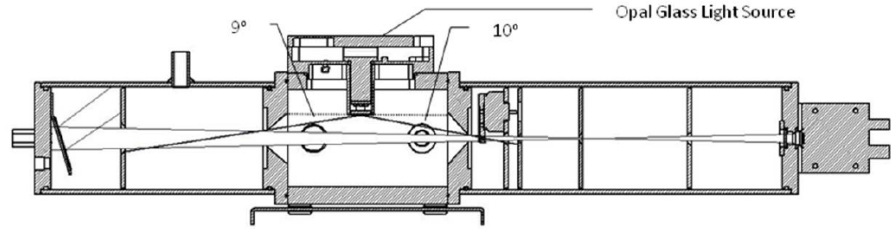

- Angular truncation

Table 2. Parameters for truncation and non-Lambertian illumination correction functions. Correction functions are given for TSI model 3563 and Aurora 3000 nephelometers.

Nephelometer	α_1	α_2	β_1	β_2	γ_1	γ_2
TSI 3563(1)	7°	170°	1.005	1. 175	73.86	32.84
Aurora 3000	10°	171°	1.01	1.190	70.25	39.99

from Müller et al., AMT, 2011

NEPHELOMETERS

from Müller et al., AMT, 2011 and Anderson and Ogren, AST, 1998

- *Angular sensitivity of nephelometers: non-Lambertian (non ideal) illumination and angular truncation*

➢ Scattering correction: $Scatt_{corr}(\lambda, t) = C(\lambda, t) \cdot Scatt_{uncorr}(\lambda, t); \qquad C(\lambda) = a + b \cdot \alpha^*(\lambda)$

Table 3b. Correction factors for total scatter as function of Ångström exponent: $C_{ts} = a + b \times \alpha^*_{ts}$. For correction of scattering coefficients for the blue (B) wavelength the Ångström exponent calculated from uncorrected scattering coefficients of blue and green (B/G) is used. At the wavelength G and R Ångström exponents at the wavelength pairs B/R and G/R are used, respectively.

	wavelength	B		G		R	
	Ångström exponents	α^*_{ts}(B/G)		α^*_{ts}(B/R)		α^*_{ts}(G/R)	
	parameters	*a*	*b*	*a*	*b*	*a*	*b*
TSI 3563	no cut	1.345	−0.146	1.319	−0.129	1.279	−0.105
	sub-µm	1.148	−0.041	1.137	−0.040	1.109	−0.033
Aurora 3000	no cut	1.455	−0.189	1.434	−0.176	1.403	−0.156
	sub-µm	1.213	−0.060	1.207	−0.061	1.176	−0.053

➢ Backscattering correction: $Back_{corr}(\lambda, t) = C(\lambda) \cdot Back_{uncorr}(\lambda, t)$

Table 3a. Nephelometer correction factors for angular nonidealities. Wavelengths for TSI 3563 are 450 nm (B), 550 nm (G), and 700 nm (R), and wavelengths for Aurora 3000 are 450 nm (B), 525 nm (G), and 635 nm (R), respectively.

(a) Midpoint ± half range of calculated correction factors for conditions with and without sub-µm cut

		backscatter		
	wavelength	B	G	R
TSI 3563	no cut	0.983 ± 0.040	0.984 ± 0.041	0.988 ± 0.043
	sub-µm	0.950 ± 0.009	0.944 ± 0.012	0.954 ± 0.009
Aurora 3000	no cut	0.963 ± 0.040	0.971 ± 0.047	0.968 ± 0.043
	sub-µm	0.932 ± 0.012	0.935 ± 0.017	0.935 ± 0.014

Calculation of Angstrom Exponents (AE) and calculation of optical measurements at other-than-measured wavelengths

The SAE and AAE describe how scattering and absorption, respectively, vary as a function of λ

Extensive optical properties

- o Scattering [m^{-1}]
- o Backscattering [m^{-1}]

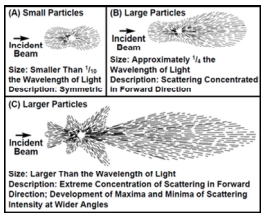

$$Scattering \propto \frac{1}{\lambda^{SAE}}$$

$$SAE = \frac{\log\left(\frac{S_{\lambda_1}}{S_{\lambda_2}}\right)}{\log\left(\frac{\lambda_1}{\lambda_2}\right)}$$

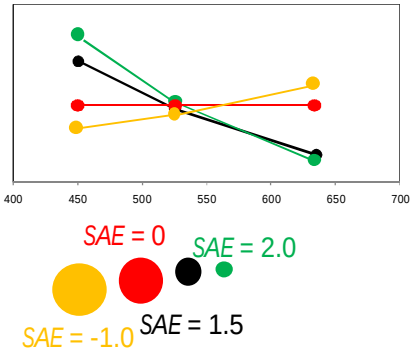

- o Scattering Ångström Exponent (*SAE*)

Extensive optical properties

- o Absorption [m^{-1}]

$$Absorption \propto \frac{1}{\lambda^{AAE}}$$

$$AAE = \frac{\log\left(\frac{A_{\lambda_1}}{A_{\lambda_2}}\right)}{\log\left(\frac{\lambda_1}{\lambda_2}\right)}$$

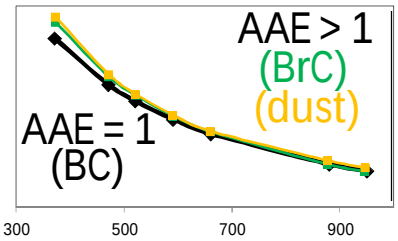

- o Absorption Ångström Exponent (*AAE*)

Calculation of Angstrom Exponents (AE) and calculation of optical measurements at other-than-measured wavelengths

The AE describes how an extensive aerosol particle optical property varies as a function of λ

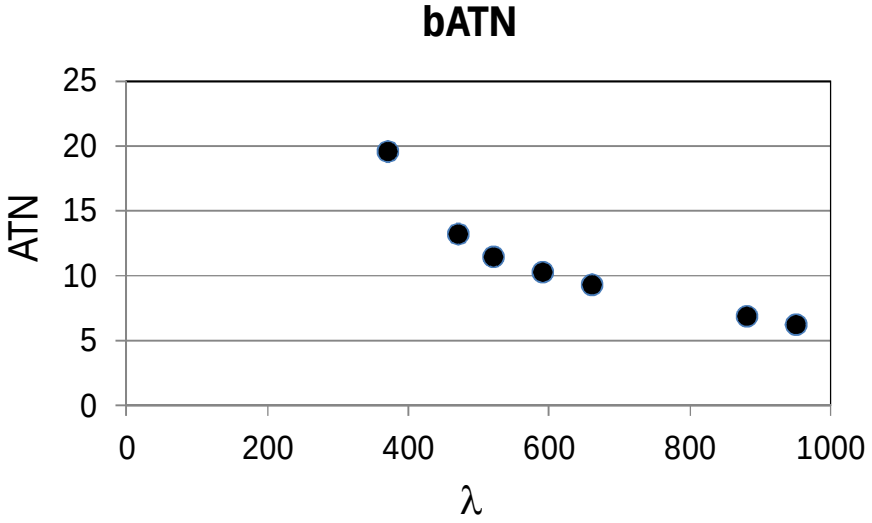

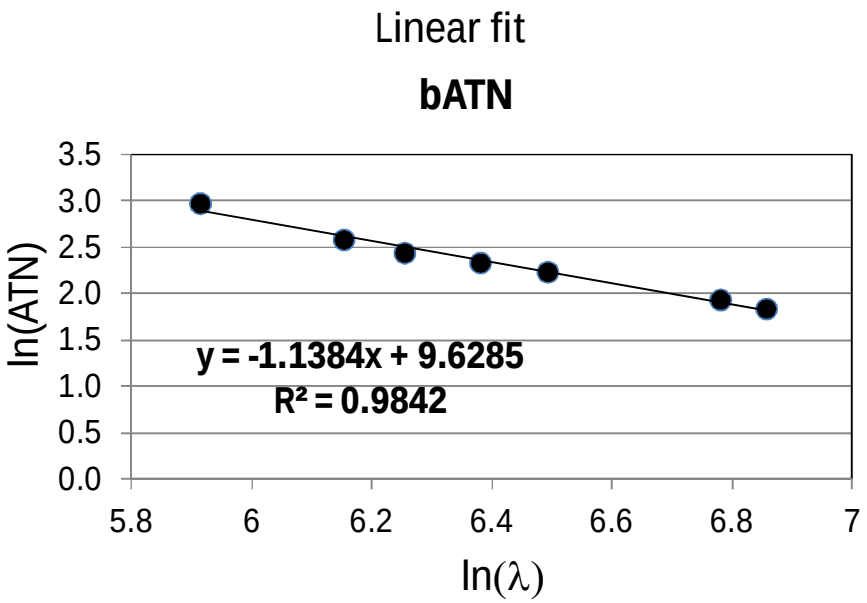

$$b_{ATN,637\ nm} = b_{ATN,660\ nm} \cdot \left(\frac{637}{660}\right)^{-b_{ATN}\ AE}$$

Calculation of Angstrom Exponents (AE) and calculation of optical measurements at other-than-measured wavelengths

The AE describes how an extensive aerosol particle optical property varies as a function of λ

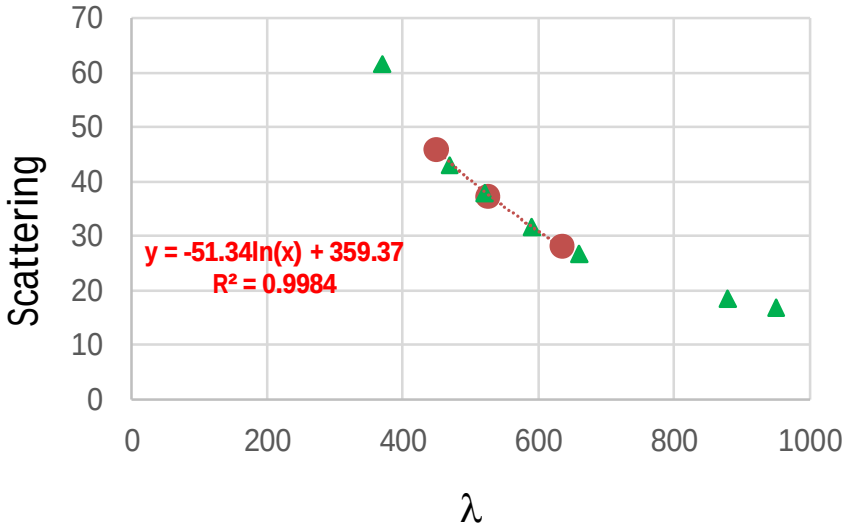

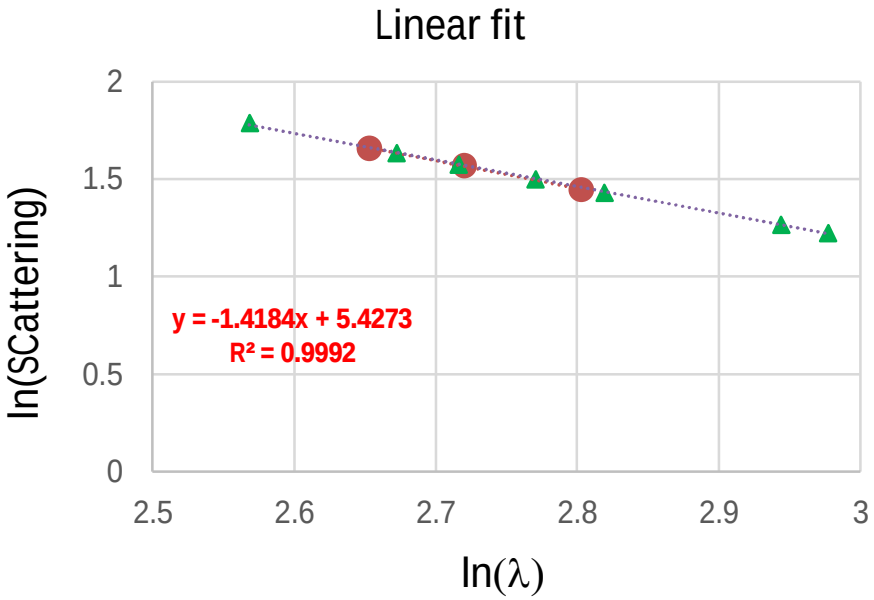

$$Scatt_{,880\ nm} = Scatt_{,635\ nm} \cdot \left(\frac{635}{880}\right)^{-SAE}$$

INTENSIVE AEROSOL PARTICLES OPTICAL PROPERTIES:

single scattering albedo

$$SSA\ (\lambda) = \frac{\sigma_{sp}\ (\lambda)}{\sigma_{sp}\ (\lambda) + \sigma_{ap}\ (\lambda)}$$

single scattering albedo Ångström exponent

$$SSAAE\ (\lambda) = -\frac{\log\left(\frac{SSA^{\lambda 1}}{SSA^{\lambda 2}}\right)}{\log\left(\frac{\lambda_1}{\lambda_2}\right)}$$

Scattering Ångström exponent

$$SAE\ (\lambda) = -\frac{\log\left(\frac{\sigma_{sp}^{\lambda 1}}{\sigma_{sp}^{\lambda 2}}\right)}{\log\left(\frac{\lambda_1}{\lambda_2}\right)}$$

Mass absorption cross section

$$MAC\ (\lambda) = \frac{\sigma_{ap}^{\lambda}}{EC}$$

Absorption Ångström exponent

$$AAE\ (\lambda) = -\frac{\log\left(\frac{\sigma_{ap}^{\lambda 1}}{\sigma_{ap}^{\lambda 2}}\right)}{\log\left(\frac{\lambda_1}{\lambda_2}\right)}$$

Mass scattering efficiency

$$MSE\ (\lambda) = \frac{\sigma_{sp}^{\lambda}}{PM}$$

SAE European phenomenology

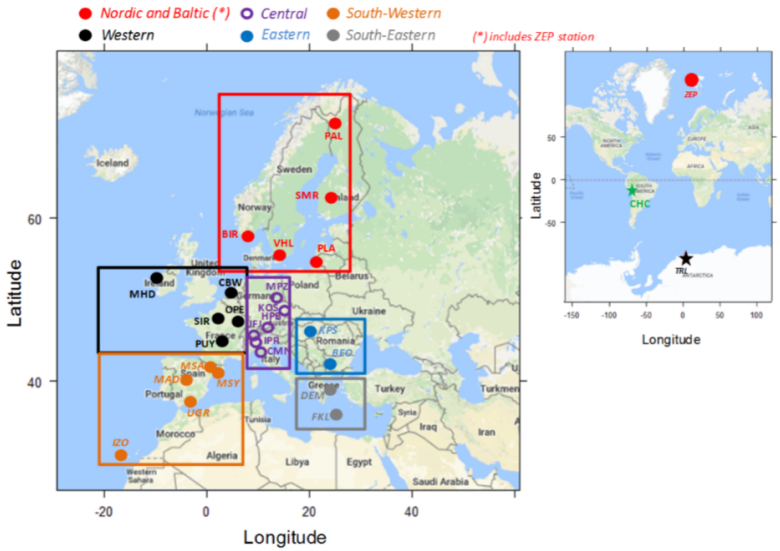

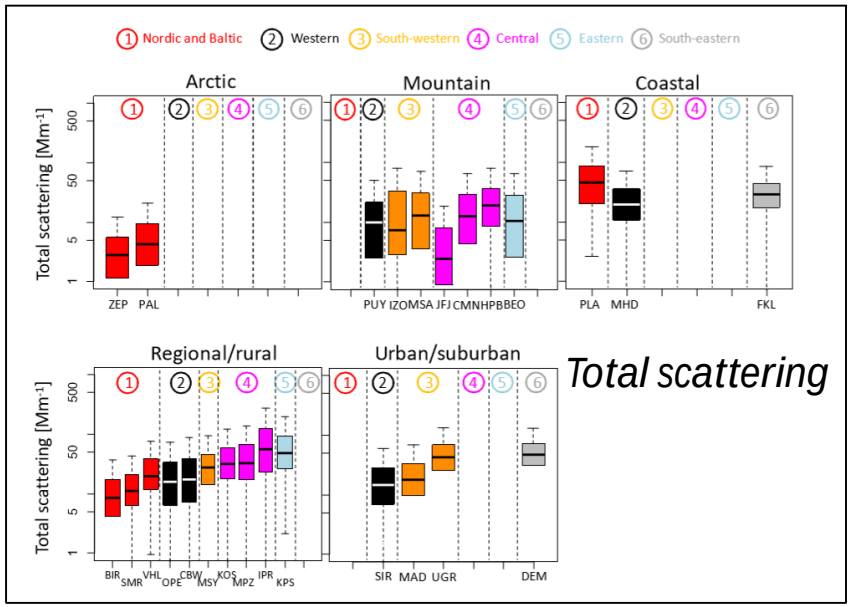

Pandolfi et al., ACP, 2018

Atmos. Chem. Phys., 18, 7877–7911, 2018
https://doi.org/10.5194/acp-18-7877-2018

Atmospheric Chemistry and Physics
Open Access
EGU

A European aerosol phenomenology – 6: scattering properties of atmospheric aerosol particles from 28 ACTRIS sites

Marco Pandolfi[1], Lucas Alados-Arboledas[2], Andrés Alastuey[1], Marcos Andrade[3], Christo Angelov[4], Begoña Artiñano[5], John Backman[6,7], Urs Baltensperger[8], Paolo Bonasoni[9], Nicolas Bukowiecki[8], Martine Collaud Coen[10], Sébastien Conil[11], Esther Coz[5], Vincent Crenn[12,13], Vadimas Dudoitis[14], Marina Ealo[1], Kostas Eleftheriadis[15], Olivier Favez[16], Prodromos Fetfatzis[15], Markus Fiebig[17], Harald Flentje[18], Patrick Ginot[19], Martin Gysel[8], Bas Henzing[20], Andras Hoffer[21], Adela Holubova Smejkalova[22,23], Ivo Kalapov[4], Nikos Kalivitis[24,25], Giorgos Kouvarakis[24], Adam Kristensson[26], Markku Kulmala[6], Heikki Lihavainen[7], Chris Lunder[17], Krista Luoma[6], Hassan Lyamani[2], Angela Marinoni[9], Nikos Mihalopoulos[24,25], Marcel Moerman[20], José Nicolas[27], Colin O'Dowd[28], Tuukka Petäjä[6], Jean-Eudes Petit[12,16], Jean Marc Pichon[27], Nina Prokopciuk[14], Jean-Philippe Putaud[29], Sergio Rodríguez[30], Jean Sciare[12,a], Karine Sellegri[27], Erik Swietlicki[26], Gloria Titos[2], Thomas Tuch[31], Peter Tunved[32], Vidmantas Ulevicius[14], Aditya Vaishya[28,33], Milan Vana[22,23], Aki Virkkula[6], Stergios Vratolis[15], Ernest Weingartner[8,b], Alfred Wiedensohler[31], and Paolo Laj[6,9,19]

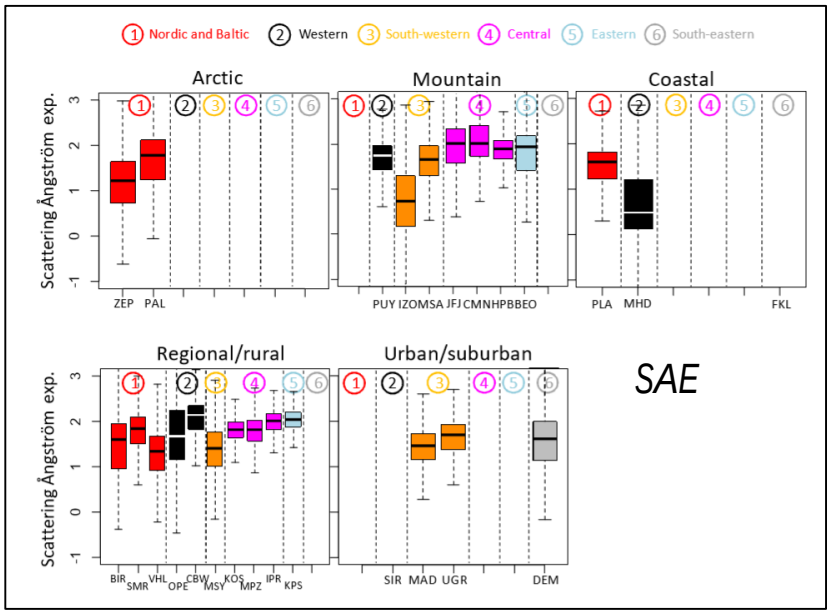

Calculation of SSA-AE: near real-time detection of dust

SSA-AE (λ) = (1-$\omega_0(\lambda)$)·(SAE(λ)-AAE(λ)) *(Moosmüller et al., ACP, 2011)*

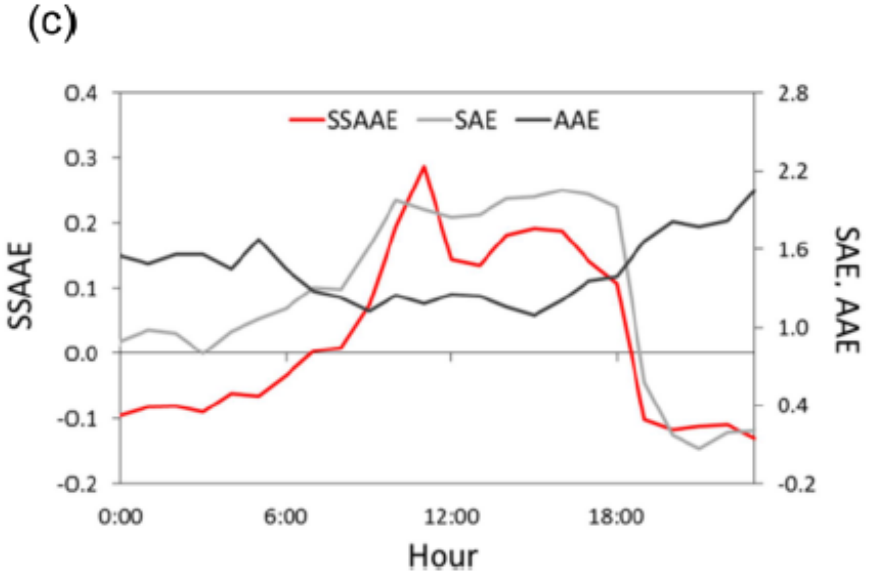

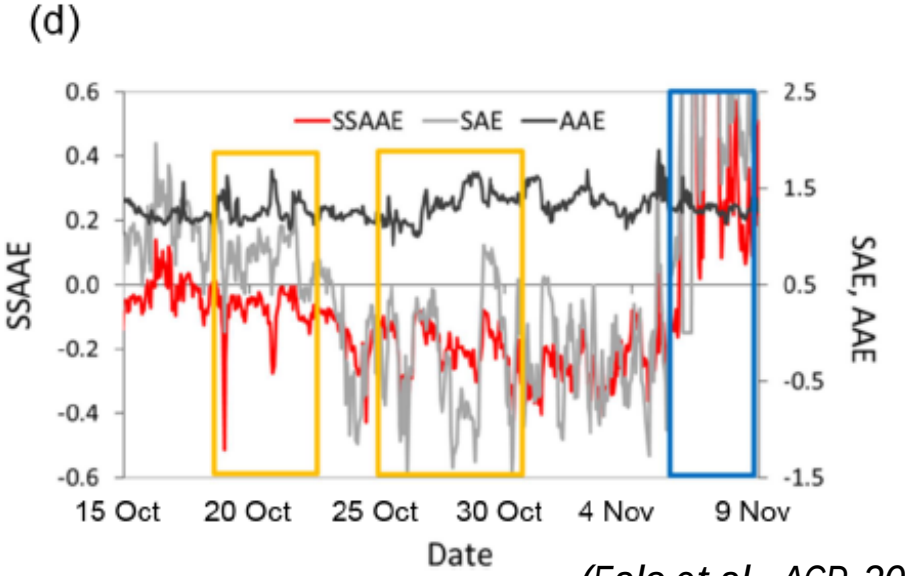

(Ealo et al., ACP, 2011)

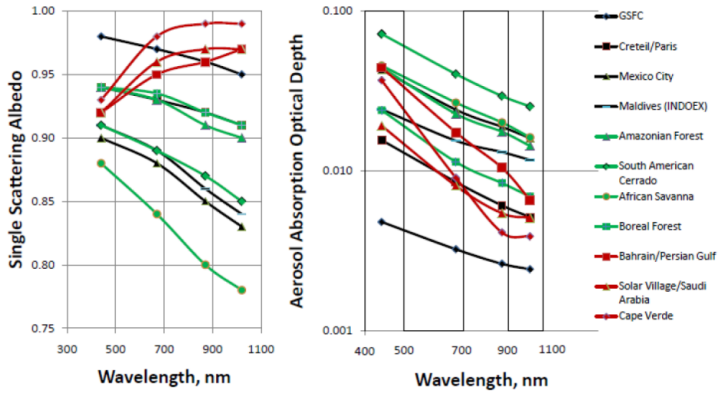

(Russel et al., ACP, 2010)

Angstrom Matrix: SAE vs AAE

(Ealo et al., ACP, 2016)

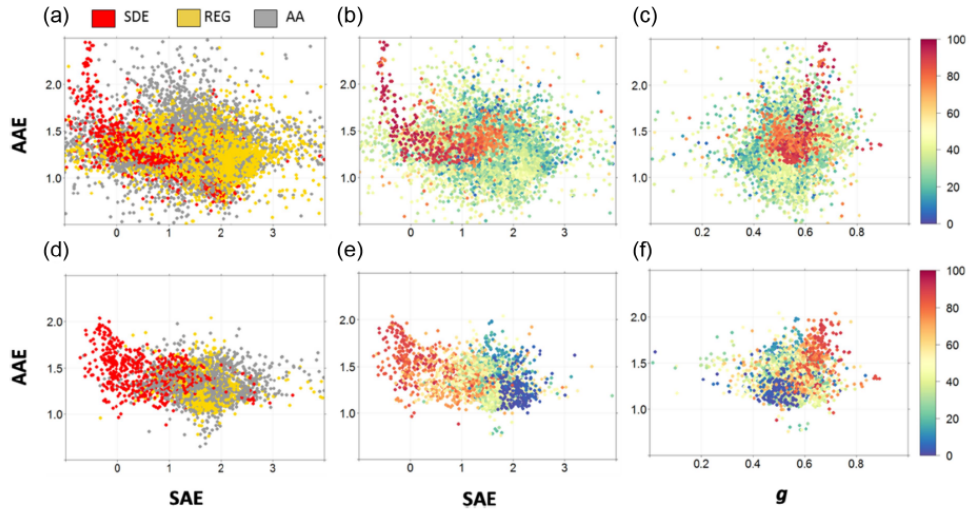

Figure 2. Ångström matrix (scatter plot of AAE vs. SAE weighted by air mass origin) at (**a**) MSY and (**d**) MSA. Ångström matrix (scatter plot of AAE vs. SAE weighted by levels of $\%PM_{1-10}$ in PM_{10}) at (**b**) MSY and (**e**) MSA. Ångström-asymmetry parameter matrix (scatter plot of AAE vs. g weighted by levels of $\%PM_{1-10}$ in PM_{10}) at (**c**) MSY and (**f**) MSA (on an hourly basis).

(Cazorla et al., ACP, 2013)

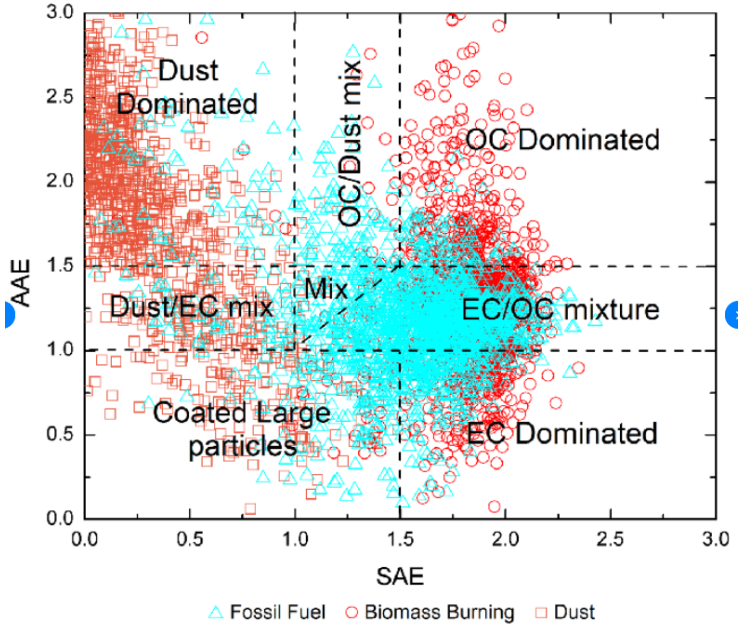

Calculation of Backscatter Fraction (BF) and Asymmetry Parameter (g)
Angular distribution of scattered light

The BF is the ratio between hemispheric backscatter and total scattering

- *The BF can be calculated from continuous measurements of Back and Scatt:*

$$BF\ (\lambda) = \frac{Back(\lambda)}{Scatt(\lambda)}$$

- *The g is defined as the intensity-weighted average cosine of the scattering angle:*

$$g = \frac{1}{2}\int_0^{\pi} \cos(\vartheta)\, P(\vartheta) sin\theta d\theta$$

g is a fundamental parameter for radiative transfer models which commonly utilize a parameterization of the angular distribution of scattered light (computationally more efficient).

$$g = -7.143889 \cdot BF + 7.464439 \cdot BF^2 - 3.96356 \cdot BF^3 + 0.9893$$

Andrews et al., 2006

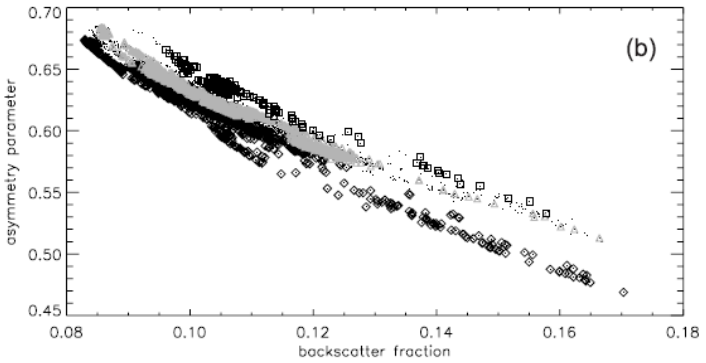

Figure 8. Importance of size distribution width. (a) Relationship between volume mean diameter and asymmetry parameter. (b) Relationship between backscatter fraction and asymmetry parameter. Data plotted are from AOS PCASP for diameter <1 μm, λ = 550 nm, and RI = 1.55 + 0.015i.

Mass Absorption Cross Section (MAC)

Measured from Absorption (MAAP) and EC (filter analysis)

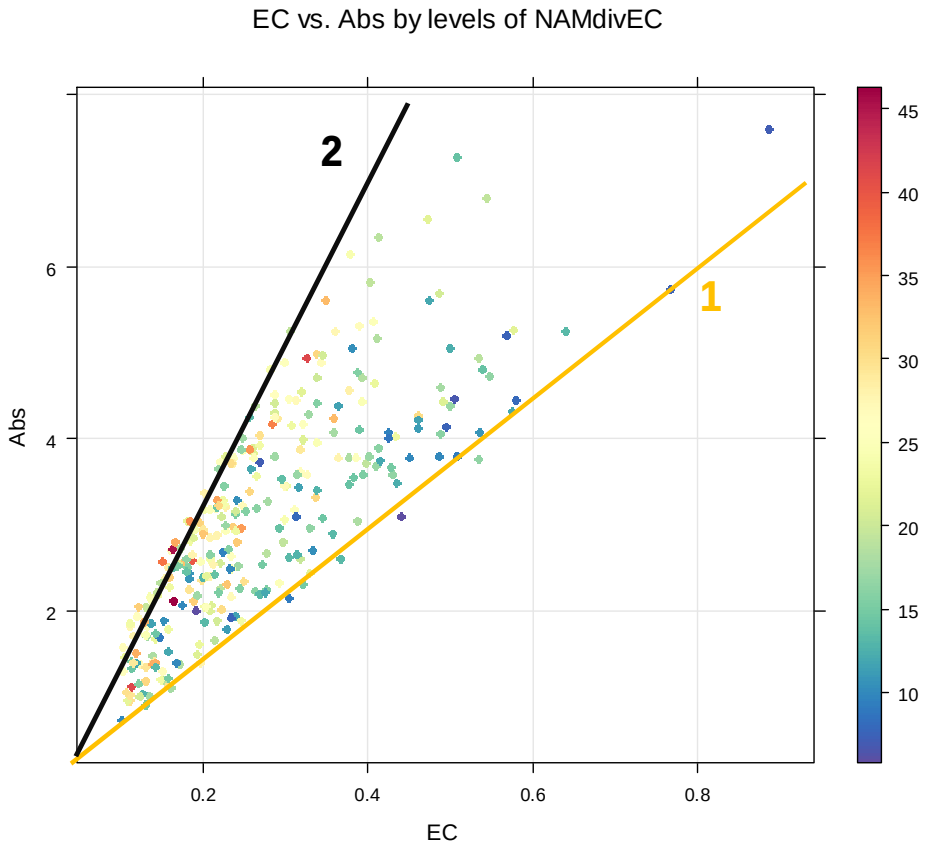

Edge 1: MAC = 6 [Mm^{-1}] / 0.8 [$\mu g/m3$] = 7.5 [m^2/g]

Edge 2: MAC = 7 [Mm^{-1}] / 0.4 [$\mu g/m3$] = 17.5 [m^2/g]

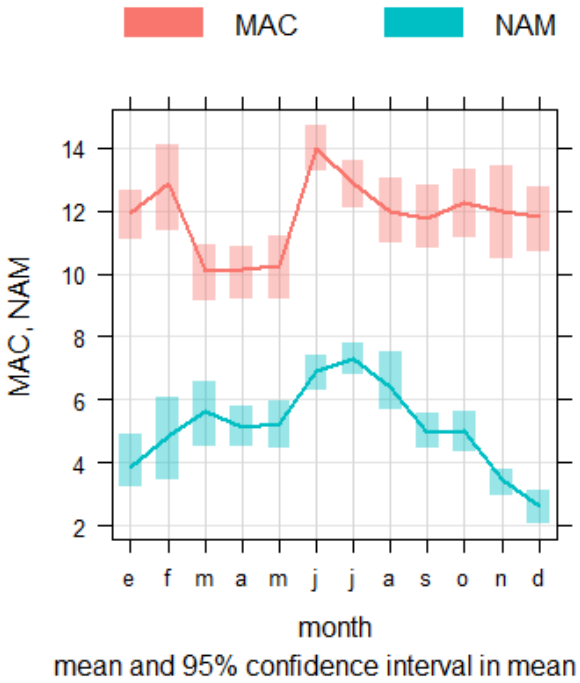

NAM = SO4-NO3-OC

Mass Absorption Cross Section (MAC)

Zanatta et al., AE, 2016

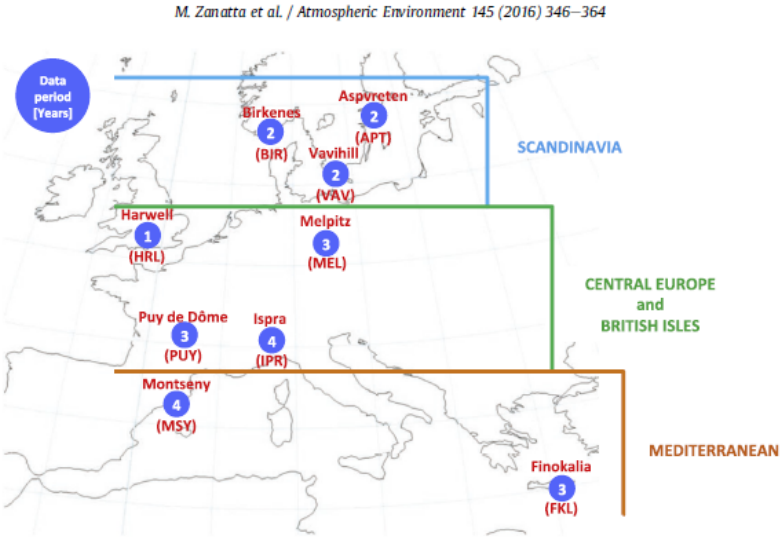

Fig. 1. Location of sampling sites and duration of measurements included in this study.

MAC

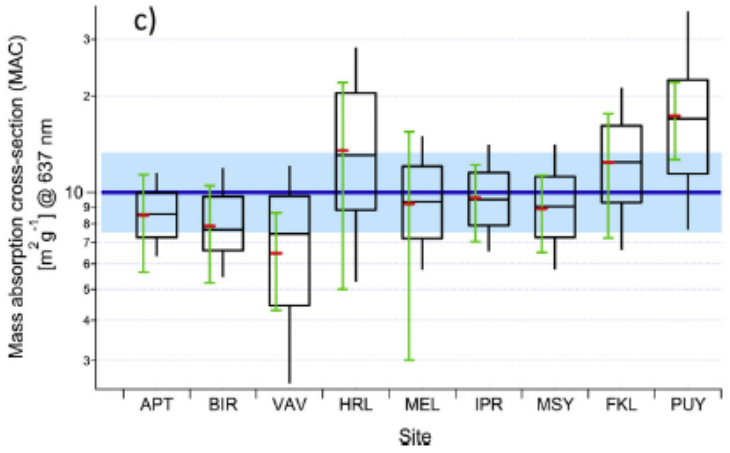

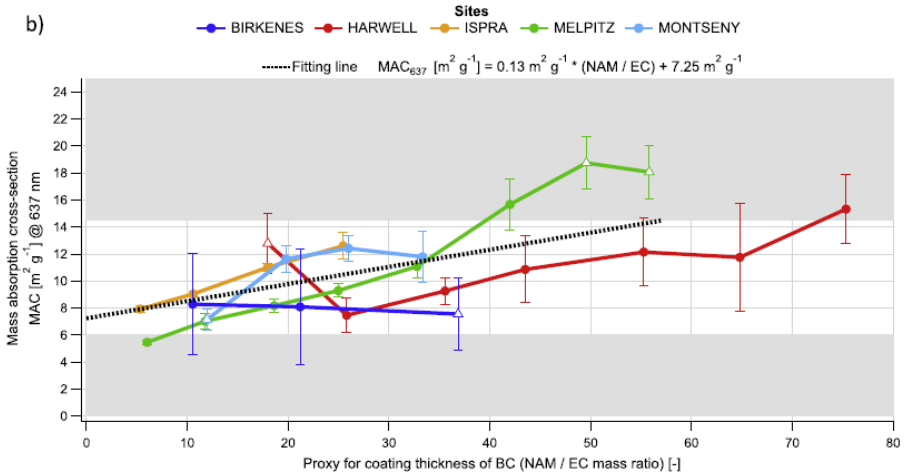

Fig. 6. a) Annual mean mass fractions of major aerosol components (organic matter, sulfate, nitrate and elemental carbon) used as input for the BC mixing state proxy. b) Dependence of the MAC on the proxy for the coating thickness, defined as the mass ratio of non-absorbing matter (NAM) to elemental carbon (EC). Individual data points were grouped into bins with different NAM to EC mass ratios. The circular markers show the mean MAC value and the mean NAM to EC mass ratio of all data points falling into the corresponding bin. Averages based on 5–10 data points only are drawn as empty triangles instead of circles. Error bars represent the standard error of the mean value. The grey shading frames the approximate range of physically reasonable MAC values calculated using Mie theory. Experimental results outside this range are likely biased due to a substantial and asymmetric contribution from outliers in the EC mass concentration and/or absorption coefficient data.

TEOM (Tapered Element Oscillating Microbalance)

▪ *Underestimation of TEOM PM compared to Reference (gravimetry) PM due to lost of semi-volatile compunds under normal operation conditions (50 °C)*

o *This underestimation also depends on the season of the year and on the study region which affect the temperature difference between ambient air and the instrument and the relative importance of non-volatile compounds in PM;*
o*The correction is also function of the aerosol precursor (α-pinene, β-pinene, limonene,.....)*

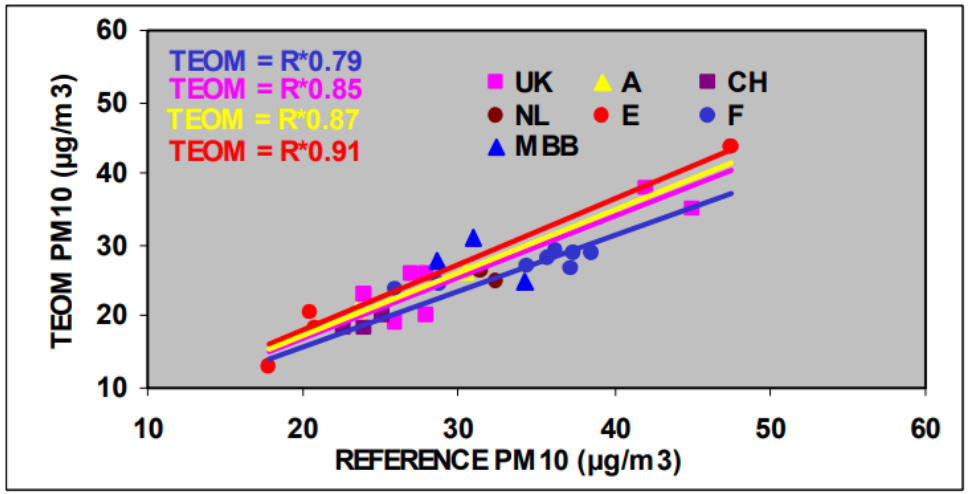

❑ *Samples at lower temperature (30ºC) by using diffusion dryer to remove water*